

---

*Research article*

## Sulfated polysaccharide-rich extract from *Navicula incerta*: physicochemical characteristics, antioxidant activity, and anti-hemolytic property

Ricardo I. González-Vega<sup>1</sup>, Carmen L. Del-Toro-Sánchez<sup>2</sup>, Ramón A. Moreno-Corral<sup>2</sup>, José A. López-Elías<sup>2</sup>, Aline Reyes-Díaz<sup>3</sup>, Norma García-Lagunas<sup>2</sup>, Elizabeth Carvajal-Millán<sup>4,\*</sup> and Diana Fimbres-Olivarría<sup>2,\*</sup>

<sup>1</sup> University of Guadalajara (UDG), Cienega University Center, Universidad Ave. 1115, Lindavista, 47820, Ocotlán, Jalisco, México

<sup>2</sup> University of Sonora (UNISON), Rosales y Niños Héroe S/N, 83000, Hermosillo, Sonora, México

<sup>3</sup> State University of Sonora (UES), Navojoa Academic Unit, Manlio Fabio Beltrones Blvd. 810, 85875, Navojoa, Sonora, México

<sup>4</sup> Research Center for Food and Development (CIAD, A.C.), Carretera Gustavo Enrique Astiazarán Rosas, 46, 83304, Hermosillo, Sonora, México

\* **Correspondence:** Email: [diana.fimbres@unison.mx](mailto:diana.fimbres@unison.mx), [ecarvajal@ciad.mx](mailto:ecarvajal@ciad.mx); Tel: +526622592136, +5266225921372892400; Fax: +526622592135, +526622800421.

**Abstract:** A sulfated polysaccharide from *Navicula incerta* (SPNi) was extracted, and its physicochemical characteristics, antioxidant activity, and anti-hemolytic property were investigated. The polysaccharide yield was 4.8% (SPNi weight/biomass dry weight). Glucose, galactose, mannose, and xylose were the primary sugars. The sulfate content and  $M_w$  values were 0.46% and 45 kDa, respectively. The FT-IR spectrum showed characteristic bands at 3276, 1079, 1255, and 820  $\text{cm}^{-1}$ , related to -OH, C-O-C, S=O, and C-O-S stretching vibration. The  $^1\text{H-NMR}$  analysis revealed signals of anomeric protons, indicating the presence of  $\text{CH}_2\text{-O}$  and  $\text{CH-O}$  groups. SPNi registered ferric-reducing antioxidant power (up to 1.47  $\mu\text{mol TE/g}$ ) and 54% anti-radical activity on  $\text{ABTS}^+$ . This polysaccharide registered 90% hemolysis inhibition achieving integrity of the erythrocyte membrane. The results indicate that SPNi could be a candidate for biotechnology applications where antioxidant activity and hemolysis inhibition are required.

**Keywords:** *Navicula incerta*; benthic diatoms; sulfated polysaccharide; antioxidant activity; anti-hemolytic property; bioactivity

---

## 1. Introduction

Benthic diatoms represent a valuable resource because of their extracellular polymeric substances. Recently, they have been of particular interest because of the bioactive properties of their sulfated polysaccharides [1,2]. To date, differences in the composition and structure of sulfated polysaccharides produced by microalgae have been observed. These molecules exist as homopolymers of galactose and glucose [3] or heteropolymers of galactose, xylose, and glucose [4] in different proportions. Furthermore, rhamnose, fructose, and uronic acids have been identified in some species of microalgae [5]. The chemical structure of polysaccharides is linked to their biological properties. The search for new bioactive compounds to prevent many diseases has recently focused on natural products, such as sulfated polysaccharides. It has been observed that sulfur-rich biopolymers play a critical role in inhibiting the activation of anti-inflammatory macrophages, at the same time promoting the proliferation and migration of endothelial cells [6]. Previous studies have demonstrated that polysaccharides from vegetal sources exhibit anti-hemolytic properties [7–9], and it has been observed that those with sulfate groups have more significant antihemolytic activity [8]. These compounds are effective against conditions associated with oxidative stress, such as inflammation and cancer. In addition, antioxidants can inhibit free radicals and prevent cell damage through anti-hemolytic activity. Currently, it has been shown that polymeric biomaterials offer a wide range of therapeutic possibilities in the field of health. Its use is not limited to molded or machined parts, but also as drug-loaded coatings, biosensors, fibers, and medical devices, among others. Systematic experiments have shown that sulfur-based biomaterials have excellent blood biocompatibility with significant antihemolytic and anti-inflammatory attributes [10]. However, the relationship between sulfated polysaccharides structure and biological activity has not been completely defined because of the complexity of these polymers [11]. To further understand their mechanism of action, it is necessary to investigate the molecular weight, chemical structure, sulfate content, and type of monosaccharides contained in these compounds since these characteristics significantly affect the biological properties of these polysaccharides [12,13]. Identifying natural sources of antioxidant compounds is of interest to prevent and treat diseases associated with oxidative stress. The *Navicula* species are characterized by a high content of sulfated polysaccharides, and it has been reported that there is a positive correlation between sulfate content and bioactivity, such as ameliorating disorders caused by oxidative stress [11]. In the present study, a sulfated polysaccharide was extracted from *Navicula incerta* (SPNi), and its physicochemical characteristics, antioxidant activity, and anti-hemolytic property were investigated. To our knowledge, this study is the first to describe the antioxidant activity of SPNi and the protective effect of this natural polymer against radical-induced oxidative stress in erythrocytes.

## 2. Materials and methods

### 2.1. Culture conditions

*Navicula incerta* (CICESE NV11) was obtained from the Collection of Marine and Freshwater Microalgae Strains of the Department of Aquaculture of the Centro de Investigación Científica y de Educación Superior de Ensenada (CICESE, Baja California, Mexico). The experiments were carried out under laboratory-controlled conditions. The “F” medium [14] was used for microalgae culture in 20 L tanks at a volume of 10 L per culture. The conditions included constant aeration at  $25 \pm 1$  °C (pH 7.0) with continuous light (24 h) to maintain the culture. The diatom was cultivated under white wavelength (400–750 nm) at  $50 \mu\text{mol photon m}^{-2} \text{sec}^{-1}$  through light-emitting diode lamps. Finally, the total biomass was harvested at the stationary phase.

### 2.2. SPNi extraction, chemical composition, and molecular weight

The sulfated polysaccharide from *Navicula incerta* was extracted as reported before [15]. The soluble sulfated polysaccharides were obtained from lyophilized microalgal biomass. 10 g of biomass were suspended in distilled water for 1 h at 30 °C and then were centrifuged for 15 min at  $20,000 \times g$ . The supernatant resultant was precipitated overnight under cold conditions with 96% (v/v) ethanol to allow for the precipitation of sulfated polysaccharides. The precipitate was recovered and dried by solvent exchange (96% (v/v) ethanol and pure acetone) to finally obtain the polysaccharide from *Navicula incerta* (SPNi). The sulfate content was analyzed using the sodium-rhodizonate method [16], and total protein content was measured using the Dumas method [17]. The monosaccharides content was analyzed by gas chromatography (Agilent HP 6890 GC Series, Santa Clara, CA, USA) [18]. The SPNi was hydrolyzed with 3 N  $\text{H}_2\text{SO}_4$  (98% v/v) at 100 °C. Inositol was added as an internal standard. Glucose, mannose, galactose, and xylose (1 mg/mL, w/v) were used as the external standards (Sigma-Aldrich, St. Louis, MO, USA). Sugars were reduced to alditol-acetates and extracted with chloroform. Finally, 5 mL of alditol-acetates were injected in a DB 225 type column (50% cyanopropylphenyl-dimethylpolysiloxane, 30 m 0.32 mm ID, 0.15 mm). The analysis conditions were injection temperature of 220 °C, detector temperature of 260 °C, and oven temperature programmed to 205 °C at 10 °C/min. The carrier gas was Nitrogen (1.0 mL/min). A flame ionization detector was used.

The molecular weight ( $M_w$ ) was analyzed by high-performance size-exclusion chromatography (HPSEC) attached to a multiangle laser-light scattering (MALLS) and refractive index (RI) detector (mini-Dawn®, Wyatt, Milford, MA, USA). The determination was performed in triplicate: 1 mg/mL (w/v) of SPNi was dissolved in 100 mM  $\text{NaNO}_3$  and filtered through a 0.2 mm membrane. Finally, the SPNi solution was injected at 25 °C. The RI increment utilized was 0.147 mL/g ( $dn/dc$ ) as reported for other *Navicula* species [19].

### 2.3. FT-IR spectroscopy

SPNi was analyzed using a Nicolet iS50 FT-IR spectrometer (Thermo Fisher Scientific, Waltham, MA, USA) coupled with an attenuated total reflection accessory at room temperature. Absorbance was measured from 4000 to  $400 \text{ cm}^{-1}$  [15].

## 2.4. <sup>1</sup>H-NMR analysis

The sample was prepared as previously reported [20] with some modifications. SPNi (5 mg) was dissolved in 500 mL deuterated water (D<sub>2</sub>O) and vortexed for 15 seconds. The <sup>1</sup>H-NMR of SPNi was obtained at 25 °C with a Bruker Advance 400 spectrometer (Bruker Mexicana, S. A. de C. V. Mexico) at 400 MHz. The signal emitted by <sup>1</sup>H-NMR was analyzed, and the chemical shifts were expressed as δ ppm values. Additionally, bioinformatic analysis was carried out to identify and assign the constituents of SPNi. Interpretations were based on previous investigations and an online HMDB (Human Metabolome Database) (<http://www.hmdb.ca/>).

## 2.5. Antioxidant activity

### 2.5.1. ABTS<sup>+</sup> [2,2'-azinobis (3-ethylbenzothiazolin)-6-sulfonic acid] free radical scavenging assay

Cationic free radical was prepared with ABTS<sup>+</sup> (7 mM) and potassium persulfate (2.45 mM) and incubated for 16 h under dark conditions. Briefly, the ABTS<sup>+</sup> solution was diluted with ethanol to obtain an absorbance of 0.7 at 734 nm. Then, 20 μL of SPNi was added to the ABTS<sup>+</sup> solution (270 μL). The absorbance was measured at 734 nm using a MULTISKAN GO spectrophotometer (Thermo Fisher Scientific Oy, Vantaa, Finland) after incubating for 30 min in the dark at room temperature. Measurements were performed in triplicate. Gallic acid was used as the positive control (100 μg/mL) [21]. The scavenging activity of ABTS<sup>+</sup> radicals by the SPNi was calculated according to the following equation:

$$\% \text{ of inhibition} = (\text{Initial absorbance} - \text{Final absorbance}) / (\text{Initial absorbance}) * 100 \quad (1)$$

### 2.5.2. FRAP (ferric reducing antioxidant power) assay

The FRAP assay was performed as described before [22] with some modifications. The stock solutions were sodium acetate buffer (300 mM, pH 3.6), FeCl<sub>3</sub> (20 mM), and TPTZ (2,4,6-tripyridyl-s-triazine) solution (10 mM) in HCl (40 mM). The FRAP working solution was prepared at a ratio of 10:1:1 (Buffer: FeCl<sub>3</sub>: TPTZ). The reactions were as follows: 20 μL of SPNi (15 mg/mL) were added to FRAP solution (280 μL) in a 96-well microplate and the absorbance was read (MULTISKAN GO, Thermo Scientific, Waltham, MA, USA). The reactions were monitored for 40 min at 10-min intervals by measuring absorbance at 638 nm in the dark at room temperature. Measurements were performed in triplicate. The results are expressed as micromole Trolox equivalents (μMol TE/g D.W.).

### 2.5.3. Anti-hemolytic activity and erythroprotective effect on AAPH- induced oxidative damage

The Red Blood Cells (RBCs) O type with RhD+ve used in the present study were donated by the Clinical Analysis Laboratory of the University of Sonora. The anti-hemolytic activity was evaluated by hemolysis caused by AAPH (2,2'-azobis-[2-methylpropionamidine]) free radicals according to the method previously reported [23]. RBCs were collected by venipuncture using a completely sterile vial and mixed with an anticoagulant (EDTA) to prevent blood clotting. The radical AAPH was prepared in phosphate-buffered saline (PBS) at a concentration of 400 mM and the pH was adjusted to 7.4. Briefly, 100 μL of RBCs, 100 μL of SPNi, and 100 μL of AAPH radical were combined. SPNi and

controls were incubated for 3 h at 37 °C with constant stirring at 30 rpm in the dark. Once the incubation was finished, the samples were diluted with PBS (1 mL) and centrifuged for 5 min at 2000 g (Heraeus Multifuge X1R, Thermo Scientific, Waltham, MA, USA). The supernatant was collected, and the absorbance was measured at 540 nm in a 96-well microplate (MULTISKAN GO, Thermo Scientific, Waltham, MA, USA). The percentage of hemolysis inhibition was calculated according to the following equation

$$\% \text{ Of hemolysis inhibition} = (AAPH1 - HM)/(AAPH1) * 100 \quad (2)$$

where *AAPH1* is the absorbance of complete hemolysis and *HM* is the absorbance of extract hemolysis.

The RBCs morphology was monitored using a compound microscope (CX23, Olympus, Shinjuku, Tokyo, JP). A drop of RBCs was placed onto a glass slide to create a thin film. Wright staining was carried out [24] to observe the damage in the erythrocyte cell membrane. The results were compared with healthy RBCs and RBCs exposed to the AAPH radical.

## 2.6. Statistical analysis

The data were analyzed by a one-way ANOVA and mean differences with Tukey's post hoc test at a confidence level of  $p \leq 0.05$  for at least three determinations ( $n \geq 3$ ). The data were analyzed using JMP version 8.0 software (SAS Institute Inc., NC, USA) [25].

## 3. Results

### 3.1. Yield and characteristics of SPNi

SPNi appeared as white solid particles. The polysaccharide yield was 4.8% (*w* SPNi/*w* *Navicula* dry weight). Gas chromatography analysis revealed the presence of four primary sugars (Table 1) with glucose (39.4%) as the most abundant monosaccharide and galactose as the second. Xylose and mannose were present as minor constituents of SPNi. A small amount of protein (3.12%) was also registered in the sample. The sulfate content was 0.46% (*w/w*) and the *M<sub>w</sub>* registered was 45 kDa.

**Table 1.** Composition of SPNi

Compound	Content
Glucose	39.40 ± 3.93
Galactose	13.88 ± 1.33
Xylose	2.290 ± 0.06
Mannose	6.190 ± 0.54
Protein	3.120 ± 0.12
Sulfate	0.460 ± 0.001

\*Note: Results are expressed in g/100 g of SPNi dry weight. Values are the mean ± standard deviation.

### 3.2. FT-IR analysis of SPNi

Seven bands were detected in the range of 3276 to 590  $\text{cm}^{-1}$  (Figure 1), the characteristic footprint of carbohydrates [7,9,26]. The strong band observed at 3276  $\text{cm}^{-1}$  corresponds to the -OH stretching vibration attributable to the hydroxyl functional group [27]. Very low intensities bands were detected at 1255 and 820  $\text{cm}^{-1}$ , corresponding to S=O and C-O-S stretching vibration, respectively [28,29]. A signal was also observed at  $\sim 590$   $\text{cm}^{-1}$  which may be assigned to an asymmetric S-O strain. A very intense band was observed at 1079  $\text{cm}^{-1}$  corresponding to a C-O-C stretching vibration related to glucoside bonds. Finally, two bands were detected in the 1640  $\text{cm}^{-1}$  and 1538  $\text{cm}^{-1}$  regions and can be attributed to amide I (-NH<sub>2</sub>) [19,30], and amide II (-NH-R) [29] vibrations.

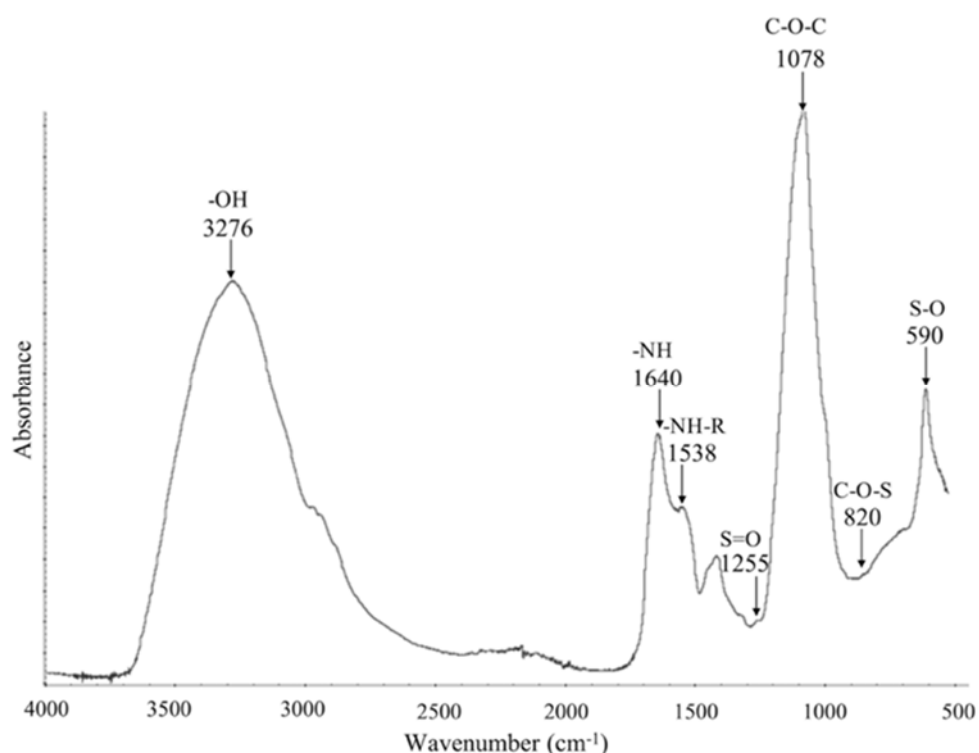


**Figure 1.** FT-IR spectrum of SPNi. The principal absorption bands are indicated.

### 3.3. <sup>1</sup>H-NMR spectroscopy

The <sup>1</sup>H-NMR spectrum of SPNi revealed many signals in the 3.2 to 5.2 ppm (Table 2) which are characteristic of polysaccharides [31–33]. SPNi exhibited two low-intensity signals at 5.2 and 4.6 ppm corresponding to the anomeric protons [34], whereas the intense signals at 3.7 and 3.2 ppm indicated the presence of CH<sub>2</sub>-O and CH-O groups [34]. Four monosaccharide residues ( $\alpha$  and  $\beta$  anomers) can be confirmed by the presence of four proton resonance signal peaks in the anomeric proton region at 4.3, 3.9, 3.7, and 3.2 ppm. Chemical shift values less than 4.0 were believed to correspond to  $\beta$ -anomeric protons while signals greater than 4.0 ppm correspond to  $\alpha$ -anomeric proton [35]. The main carbohydrates identified in SPNi by <sup>1</sup>H-NMR were glucose, galactose, xylose, mannose, and rhamnose.

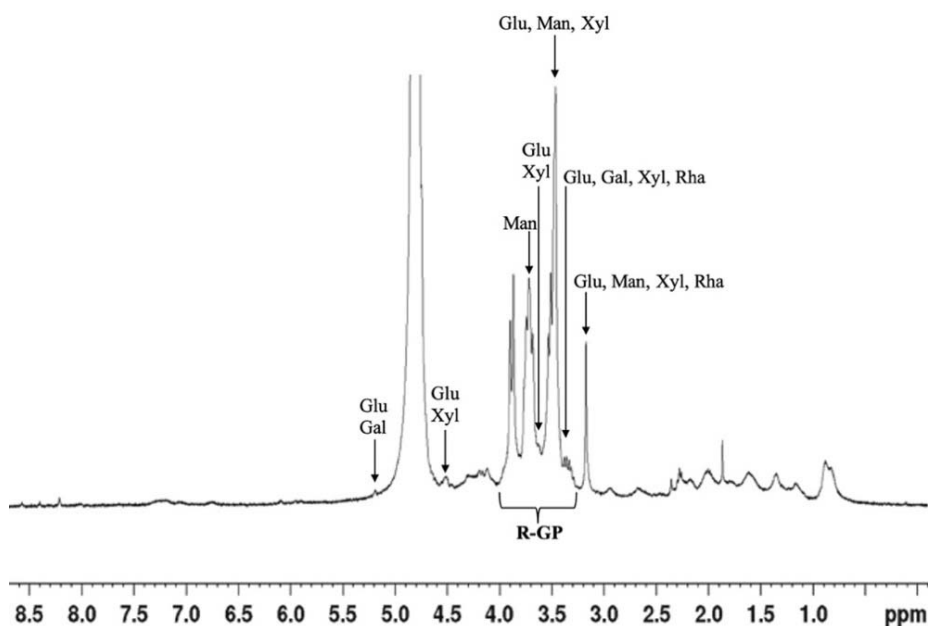


**Figure 2.**  $^1\text{H-NMR}$  spectrum of extracellular sulfated polysaccharide from *Navicula incerta* in  $\text{D}_2\text{O}$  solution. R-GP= Region of Glycoside Peaks. Glu: Glucose, Man: Mannose, Xyl: Xylose, Gal: Galactose, and Rha: Rhamnose.

**Table 2.** Peak assignments for the signals identify in SPNi.

Region	Peaks	$\delta$ ppm	Neutral Sugar	Reference No.
R-GP	1	3.2344	Glucose, Xylose	[34,36]
	2	3.3652	Mannose, Rhamnose	[34]
	3	3.4098	Glucose, Galactose, Xylose, Rhamnose	[34,37]
	4	3.4312	Glucose, Galactose	[34,37]
	5	3.5247	Glucose, Xylose	[34,36]
	6	3.5841	Glucose, Mannose	[34]
	7	3.6193	Glucose, Xylose	[34,36]
	8	3.6432	Glucose, Xylose	[34,36]
	9	3.7067	Mannose	[34]
	10	4.6	Glucose, Xylose	[34,36]
	11	5.2	Glucose, Galactose	[34,37]

\*Note: R-GP= Region of Glycoside Peaks. The SPNi were dissolved in  $\text{D}_2\text{O}$ .

### 3.4. Antioxidant activity

The FRAP assay is an electron transfer-based method that measures the reduction of  $\text{Fe}^{3+}$  to intensely  $\text{Fe}^{2+}$  by antioxidants in acidic media. Figure 3A shows the increase in ferric reduction from 10 to 40 min using a SPNi at 15 mg SPNi/mL in a range of concentrations from 1.15 to 1.47  $\mu\text{mol TE/g D.W}$ .

The percentage of  $\text{ABTS}^{\cdot+}$  radical inhibition by SPNi is presented in Figure 3B. The highest

percentage of ABTS<sup>+</sup> radical inhibition was  $54.49 \pm 0.67\%$  at 15 mg SPNi/mL and the IC<sub>50</sub> calculated as  $12.52 \pm 0.17$  mg/mL. However, the gallic acid achieved  $92.37 \pm 1.34\%$  of inhibition.

Concerning anti-hemolytic activity of SPNi against the free radical generator, AAPH, the highest value was registered at 15 and 30 mg/mL ( $85.6 \pm 1.4\%$  and  $89.6 \pm 1.3\%$ , respectively) (Figure 3C) with an IC<sub>50</sub> of  $1.97 \pm 0.05$  mg/mL.

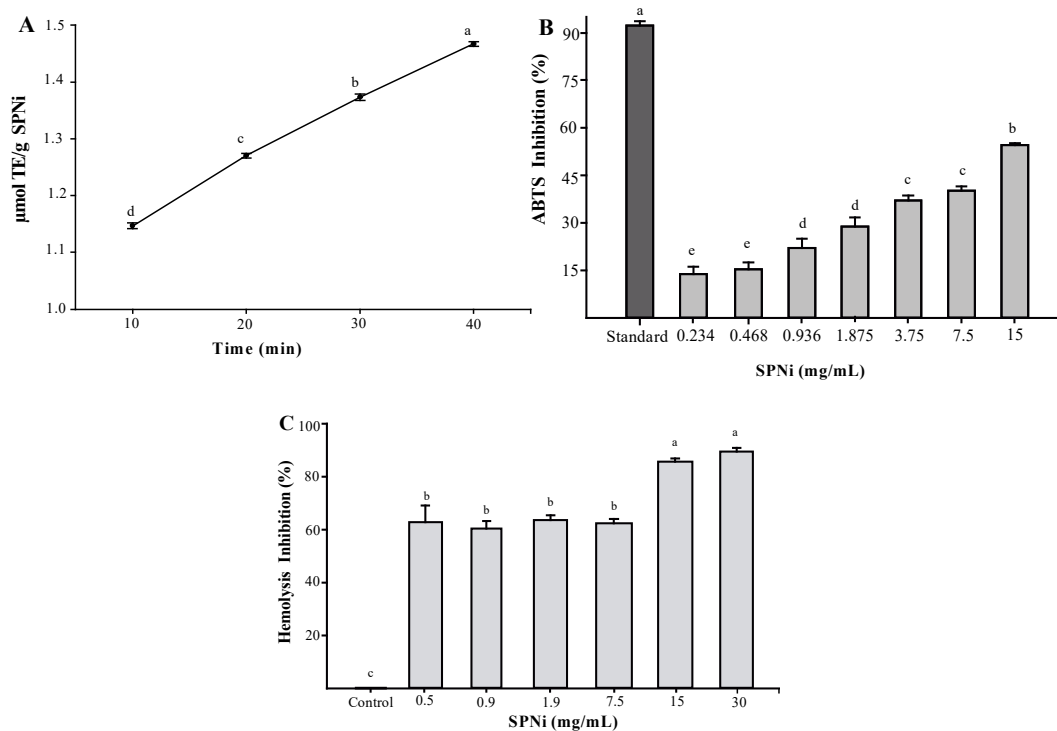


**Figure 3.** Antioxidant activity of SPNi. (A) Reducing power by FRAP at different times (min) expressed as  $\mu\text{mol}$  Trolox equivalent/g ( $\mu\text{mol TE/g D.W.}$ ), (B) Free radical scavenging by ABTS<sup>+</sup> inhibition (%) assay and (C) Hemolysis inhibition (%) at different concentrations (mg/mL). Gallic acid ( $100 \mu\text{g/mL}$ ) was used as standard in the ABTS inhibition assay. The control used in the hemolysis inhibition assay was a mixture of free radical generator AAPH and RBCs. The data represent the mean  $\pm$  standard deviation. Different letters indicate significant differences ( $p \leq 0.05$ ).

The optical micrographs of healthy RBCs revealed a typical erythrocyte morphology (Figure 4a) with a biconcave shape and depressed central zone due to the absence of a nucleus. In contrast, the cellular morphology in erythrocyte + AAPH radical (Figure 4b) exhibited an irregular shape and lysis of the membrane. Lipid peroxidation was evident, membrane degradation caused cell lysis, and hemoglobin and substances were released from the cytoplasm. The peroxy radical oxidized the cell membrane causing cell disruption. Finally, RBCs + AAPH radical treated with SPNi (Figure 4c) showed a typical erythrocyte morphology, with a regular membrane shape, visually demonstrating adequate protection. Nevertheless, the concave area of the erythrocyte membrane in Figure 4c shows slight alterations that could be interpreted as indicative of disturbance induced by oxidative treatment.



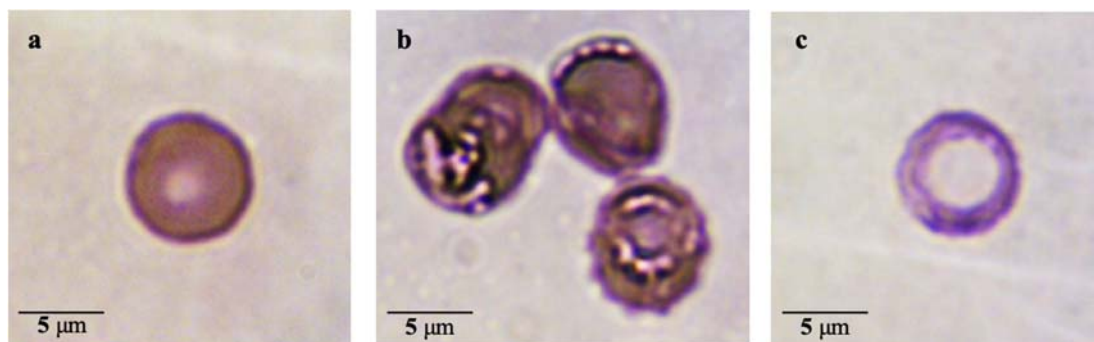


**Figure 4.** Optical micrograph of (a) erythrocyte: negative control, (b) erythrocyte + AAPH radical: positive control and (c) erythrocyte + AAPH radical + SPNi: treatment. Magnification x100, scale bar 5  $\mu\text{m}$ .

#### 4. Discussion

Sulfated polysaccharides are complex polymer compounds [38]. They consist of long-chain units of more than five neutral monosaccharides, such as repeating units of glucose, galactose, arabinose, mannose, and fucose. Still, their overall composition depends on the species and genus of the microalgae [39,40]. In addition, the concentration and composition of these biomacromolecules also rely on their physiological performance and abiotic stress (nutrient-limited medium and light conditions) [41,42]. The characteristics of these macromolecules may be responsible for various biological activities [38].

Regarding the characteristics of SPNi, glucose was the main sugar present. Diatoms are characterized by the production of silica cell walls called frustules, constituted by a complex network of polysaccharides containing glucose and mannose as the main components and proteins that regulate frustule synthesis [43]. The glucose content found in the present study is similar to that reported for *N. salinarum* (41.6%) [2] and higher than that reported for *Navicula* sp. (15%–29%) [19]. Concerning protein content, the small amount registered (3.12%) was higher than that reported for *Navicula* sp. (0.5%–1.6%) [19] but lower than that reported for other *Navicula* species [2,44]. As mentioned above, the amount of protein detected in SPNi may result from their association with cell wall polysaccharides [43]. In general, the protein content of the polysaccharides extracted from diatoms can vary from 0%–to 30% [45]. The sulfate content (0.46%) was similar to that previously reported for *Navicula* sp. (0.3%–0.4%) [19]. SPNi presented a  $M_w$  of 45 kDa. Previous studies have found that the sulfated polysaccharide from *Navicula* sp. possesses varying molecular weights when cultivated under stressful light conditions and low  $M_w$  (17 kDa) when exposed to white light [19].

FT-IR is a tool widely used to identify polysaccharides produced by different algae and microalgae [46,47]. All the bands detected in the SPNi (3276 to 590  $\text{cm}^{-1}$ ) (Figure 1) have been reported for many sulfated polysaccharides from microalgae and seaweeds [19,48–51]. The -OH stretching vibration is attributable to the hydroxyl functional group, which is a characteristic of organic compounds, such as R-OH, in which they are attached to aliphatic hydrocarbons. Some sulfated polysaccharides, such as carrageenan [52], fucoidan [53], galactan, and (1,3)- $\beta$ -D-galactan [27], contain  $\text{CH}_2\text{OH}$  and -OH groups, which are compounds produced by seaweed. The bands detected at 1255 and 820  $\text{cm}^{-1}$  correspond to the asymmetric and symmetric stretching vibration from S=O and

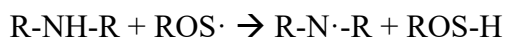
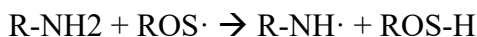
C-O-S, respectively. According to a previous study [28], the signals at  $\sim 820\text{ cm}^{-1}$  could be attributable to protons belonging to glycosidic bonds in the  $\beta$  configuration (*i.e.*, polysaccharides that contain sulfated C-O-S groups in their structure will be in the  $\beta$  configuration). However, this value is very close to the  $\alpha$ -glycosidic bonds in the anomeric region of  $842\text{ cm}^{-1}$  [29]. The low intensity at  $\sim 590\text{ cm}^{-1}$  can be attributed to the sulfate content detected in SPNi (Table 1). The band observed at  $1079\text{ cm}^{-1}$  corresponds to a C-O-C stretching vibration related to glucoside bonds. The bands seen in the  $1640\text{ cm}^{-1}$  and  $1538\text{ cm}^{-1}$  regions are typical signals for proteins and can be attributed to amide I (-NH<sub>2</sub>) [19,30], and amide II (-NH-R) [29] vibrations. The amide group I may also belong to other compounds that contain nitrogen in their structure, such as amino acids, vitamins, N-acetylglucosamine, and some polysaccharides. For this reason, the amide I functional group could be part of SPNi [54]. FT-IR spectra indicate a complex structure in SPNi [38,55–57].

<sup>1</sup>H-NMR spectroscopy is an accurate method for analyzing the structural characteristics of extracellular sulfated polysaccharides from seaweed and microalgae [58]. The <sup>1</sup>H-NMR spectrum of SPNi (Figure 2) was similar to that of the algae *Sargassum henslowianum*, *Fucus vesiculosus* [59], and *Sargassum vulgare* [13]. As mentioned, the <sup>1</sup>H-NMR spectrum of SPNi revealed many signals in the 3.2 to 5.2 ppm (Table 2). It has been reported that most of the  $\beta$ -anomeric protons are in the 4–5  $\delta$  ppm range [31]. SPNi exhibited a clear anomeric proton signal at  $\delta\text{H}$  4.6 ppm, corresponding to glucose and/or xylose [36]. In contrast, the signal at  $\delta\text{H}$  5.2 may be attributed to the anomeric proton of galactose and/or glucose [37].

The chemical structure of polysaccharides is linked to their biological properties. The search for new bioactive compounds to prevent many diseases has recently focused on natural products, such as sulfated polysaccharides. These compounds are effective against conditions associated with oxidative stress, such as inflammation and cancer. Antioxidants can inhibit free radicals and are effective and efficient at attenuating cell aging.

There is increased interest in studying marine sulfated polysaccharides because of their biological properties, such as antioxidant, anti-inflammatory, and anti-tumor activities [60]. The antioxidant activity of polysaccharides from many micro and macroalgae has been reported [61,62]; however, the antioxidant capacity of sulfated polysaccharides from *N. incerta* has not been evaluated. In the present study, the SPNi showed low reducing power. In general, it has been observed that sulfated polysaccharides from algae and microalgae lack the capacity to donate electrons and to cause a reduction from an oxidized to a reduced state [63,64]. This behavior may result from low sulfate content and protein-carbohydrate interactions that interfere with the electron transfer mechanism, which is responsible for reducing power [65]. Because the amino groups of proteins bind to the reducing end of the polysaccharides, the protein-carbohydrate interaction could reduce the biological activity of these molecules by steric hindrance of the protein [66], which would render SPNi less sensitive in the FRAP assay. Three mechanisms are generally described to account for the free radical-scavenging mechanism by sulfated polysaccharides. Single Electron Transfer followed by Proton Transfer (SET-PT), Hydrogen Atom Transfer (HAT), and Sequential Proton Loss Electron Transfer (SPLET) [67]. Under this context, the bands observed at  $3276\text{ cm}^{-1}$ ,  $1640\text{ cm}^{-1}$ , and  $1538\text{ cm}^{-1}$  regions by FT-IR corresponds to the amide I (-NH<sub>2</sub>), and amide II (-NH-R), and -OH could be responsible for transporting the electron by hydrogen atom transfer (HAT). Therefore, the following reactions can be carried out:





FRAP is an assay used to measure the reducing capacity of antioxidant molecules and is based on a SET mechanism. The FRAP assay only reflects the reducing capacity, therefore, it does not identify potential antioxidant molecules that possess HAT mechanisms as free radical scavengers. Another limitation is around potentially important antioxidants that contain thiol groups (-SH), or functional groups formed by sulfur atoms (such as S=O and C-O-S). Therefore, FRAP does not measure the potentially important antioxidant components containing -SH, S=O, and C-O-S groups, components present in the SPNi detected by FT-IR. This is mainly due to the redox potential that is below its detection. Since most SPNi components are antioxidant activity by hydrogen donation; where HAT-based assays such as ABTS, DPPH, and AAPH quantitatively better describe the antioxidant activity of SPNi. Finally, hydroxyl and thiols functional groups, traditionally called analogs of hydroxyl groups, are found based on HAT mechanisms, antioxidant molecules present in SPNi, thus, it is easier to donate protons than electrons (e<sup>-</sup>). The tentative structures lack double bonds, facilitating the electron donation mechanism (SET, Single Electron Transfer) [68,69]. SPNi lacks this characteristic and does not contain the minimum energy required to separate e<sup>-</sup> in its ground state at the highest energy level (i.e., the ionization potential is less than that required for the SET mechanism to take place) [70]. The results of the present study suggest that SPNi does not have enough groups with the ability to donate electrons; thus, the molecule can stabilize free radicals through the Hydrogen Atom Transfer (HAT) mechanism. A previous study demonstrated that the inhibition of free radicals increased with decreased sulfate content and low *M<sub>w</sub>* of sulfated polysaccharide [71]. The predominant free radical-scavenging mechanism for the cationic radical ABTS<sup>+</sup> is SET, but it can also occur by HAT, depending on the characteristics of the antioxidant and its functional groups. In this case, the predominant groups is -OH. Proton transfer involves the enthalpy of bond dissociation, which is the strength of a chemical bond. The lower the dissociation force, the greater the probability of HAT [61,72].

The results of anti-hemolytic activity of SPNi against AAPH (Figure 3) are better than that reported for aqueous extracts of *Halimeda opuntia* (82%), which exhibited an IC<sub>50</sub> of 1.25 mg/mL [73]. Few studies evaluating biological compounds from algae on hemolysis in human erythrocytes exist in the literature [73]. To our knowledge, this study is the first to describe the protective effect of SPNi against AAPH-induced oxidative stress in erythrocytes. Previous studies examined the ability of marine-origin compounds, such as pigments and SP, to inhibit AAPH-induced peroxidation on the erythrocyte membrane [13,49,74–76]. The reaction between molecular nitrogen and carbon radicals produces peroxy radicals in contact with molecular oxygen, which is derived from the degradation of AAPH. As a result, it disrupts the erythrocyte membrane causing lipid peroxidation, which is susceptible to oxidation because of its lipid nature [77,78]. Changes in cell morphology and destabilization are indirectly evident since oxidation generates holes in the membrane, expelling hemoglobin that is detectable by spectrophotometry [79]. This process can be avoided in the presence of free radical scavenger antioxidant molecules. However, on occasions, erythrocytes subjected to free radicals-induced oxidative stress and antioxidants (as an oxidative inhibitor) usually present a characteristic membrane depression (biconcavity). This usually appears slightly larger than normal without showing apparent damage to the erythrocyte membrane. This alteration could be interpreted as indicative of disturbance induced by oxidative treatment in erythrocytes. These alterations could occur because of exposure to oxidative stress induced by free radicals; where protein-l-isoaspartate (D-aspartate) O-methyltransferase

(PCMT; EC 2.1.1.77) catalyzes the esterification of the free  $\alpha$ -carboxyl group and the formation of methyl esters in the transmembrane proteins of erythrocytes. In this case, this process does not compromise cell integrity and functionality as an inhibitor of cell stress [80].

A probable anti-radical mechanism found in SPNi is based on functional groups elucidated by spectroscopy. The anti-hemolytic activity of SPNi may be attributed to the hydroxyl system and sulfated groups, part of the hydrocarbon body of polysaccharides, that transfer hydrogen atoms and stabilize the free radical species ( $\text{ROO}\cdot + \text{AOX-H} \rightarrow \text{ROOH} + \text{AOX}\cdot$ ). The SPNi effects may be due to the affinity of the radicals generated by the AAPH molecule [81]. The erythroprotective effect of SPNi against oxidative damage induced by AAPH was monitored through morphological changes to confirm the state of the membranes.

The interaction of ROS with the lipid membrane results in oxidation that affects its stability [77]. Free radical-induced eryptosis was observed in the positive control and detected by the release of hemoglobin [75]. These results suggest that SPNi has a high erythroprotective effect on healthy cells at the concentrations used in the present study. The presence of SPNi maintained membrane integrity and inhibited AAPH-induced peroxy radicals. Inhibition of the oxidation reaction prevented ROS interaction with the lipid membrane and entry into the cell. In addition to the type of inhibition mechanism (HAT), SPNi inhibited radicals in two ways: (1) in the extracellular area of the erythrocytes (before the radicals contact the membrane) and (2) binding to surface antigens, such as those of the ABO and RhD system, to exert activity directly by interacting with the cell membrane. However, the interactions described above have not been confirmed, but the interactions may be measured by the RhD+ve antigen since only the O type with RhD+ve was used in this study. This result suggests that further studies are needed on different blood groups in the ABO and Rh systems to determine if there are significant differences between the erythroprotective effects and the surface antigens.

The ability of SPNi to donate electrons or protons may be dependent upon its composition since the molecule exerts reducing activity against oxidant molecules. The anti-radical activity on  $\text{ABTS}^+$  and AAPH may be attributed to the bands detected in the FT-IR ( $-\text{OH}$ ,  $\text{S}=\text{O}$ ,  $\text{C}-\text{O}-\text{S}$ ,  $-\text{NH}$ , and  $-\text{NH}_2$ ) (Figure 1) and the functional group ( $-\text{OH}$ ) detected by  $^1\text{H}$  NMR. For this reason, the SET mechanism was not powerful enough, according to the FRAP results. Nevertheless, SPNi stabilized the radical  $\text{ABTS}^+$  through the HAT mechanism. The antioxidant mechanisms could be directly influenced by protein-carbohydrate interactions, thus enabling the  $\text{ABTS}^+$  and AAPH-induced radicals to act as proton scavengers. The interaction is likely influenced by the exposure of amino acids and sulfate groups capable of donating protons. In other words, the radical does not utilize the electron acceptor pathway. Therefore, the HAT mechanism is predominant for SPNi compared with the SET mechanism (Figure 3). This information will be helpful in future studies on the prevention of cancer cell proliferation.

## 5. Conclusions

*Navicula incerta* contains a sulfated polysaccharide that exhibits antioxidant and anti-hemolytic properties. The SPNi free radicals scavenging capacity inhibit the disruption of the erythrocyte's lysosomal membrane. The biological activity of SPNi could be partly attributed to the sulfate group content. The SPNi antioxidant activity occurs through a Hydrogen Atom Transfer (HAT) mechanism. Protein-carbohydrate interactions may directly influence this activity, but it is necessary to conduct additional studies to confirm this premise. In addition, this is the first study to demonstrate anti-

hemolytic activity and protective effects of microalgae compounds on human erythrocytes. SPNi may be a promising alternative for biotechnological applications, especially those related to human health, where antioxidant activity and prevention of chronic-degenerative diseases are needed.

## Acknowledgments

This research received funding from CONACYT, grant number 319684. The authors are pleased to acknowledge the DICTUS, CIAD, DIPA, and DIPM spectroscopy laboratory of Universidad de Sonora for use of the facilities to characterize the material.

## Conflict of interest

All authors declare no conflicts of interest in this paper.

## Author contributions

Ricardo I. González-Vega: Conceptualization, methodology, formal analysis, investigation, writing—review and editing, visualization, supervision. Carmen L. Del-Toro-Sánchez: resources, writing—review and editing. Ramón A. Moreno-Corral: methodology, writing—review and editing. José A. López-Elías: resources, writing—review and editing. Aline Reyes-Díaz: methodology, writing—review and editing. Norma García-Lagunas: formal analysis, writing—review and editing. Elizabeth Carvajal-Millán: Supervision, Project administration, Funding acquisition, Conceptualization, Writing- Reviewing and Editing, Validation. Diana Fimbres-Olivarría: Conceptualization, methodology, investigation, writing—original draft preparation, writing—review and editing, visualization, supervision.

## References

1. Raposo MF de J, de Morais RMSC, de Morais AMM (2013) Bioactivity and applications of sulphated polysaccharides from marine microalgae. *Mar Drugs* 11: 233–252. <https://doi.org/10.3390/md11010233>
2. Staats N, De Winder B, Stal LJ, et al. (1999) Isolation and characterization of extracellular polysaccharides from the epipelagic diatoms *Cylindrotheca closterium* and *Navicula salinarum*. *Eur J Phycol* 34: 161–169. <https://doi.org/10.1080/09670269910001736212>
3. Yim JH, Kim SJ, Ahn SH, et al. (2007) Characterization of a novel bioflocculant, p-KG03, from a marine dinoflagellate, *Gyrodinium impudicum* KG03. *Bioresour Technol* 98: 361–367. <https://doi.org/10.1016/j.biortech.2005.12.021>
4. Nomoto K, Yokokura T, Satoh HMM (1983) Antitumor activity of chlorella extract, PCM-4, by oral administration. *Cancer Chemother* 10: 781–785.
5. Yim JH, Kim SJ, Ahn SH, et al. (2004) Antiviral effects of sulfated exopolysaccharide from the marine microalga *Gyrodinium impudicum* strain KG03. *Mar Biotechnol* 6: 17–25. <https://doi.org/10.1007/s10126-003-0002-z>

6. Yu Y, Zhu S, Hou Y, et al. (2020) Sulfur contents in sulfonated hyaluronic acid direct the cardiovascular cells fate. *ACS Appl Mater Interfaces* 12: 46827–46836. <https://doi.org/10.1021/acsami.0c15729>
7. Feriani A, Tir M, Hamed M, et al. (2020) Multidirectional insights on polysaccharides from *Schinus terebinthifolius* and *Schinus molle* fruits: Physicochemical and functional profiles, in vitro antioxidant, anti-genotoxicity, antidiabetic, and antihemolytic capacities, and in vivo anti-inflammatory and anti-nociceptive properties. *Int J Biol Macromol* 165: 2576–2587. <https://doi.org/10.1016/j.ijbiomac.2020.10.123>
8. Meng Q, Chen F, Xiao T, et al. (2019) Inhibitory effects of polysaccharide from *Diaphragma juglandis fructus* on  $\alpha$ -amylase and  $\alpha$ -D-glucosidase activity, streptozotocin-induced hyperglycemia model, advanced glycation end-products formation, and H<sub>2</sub>O<sub>2</sub>-induced oxidative damage. *Int J Biol Macromol* 124: 1080–1089. <https://doi.org/10.1016/j.ijbiomac.2018.12.011>
9. Duan S, Zhao M, Wu B, et al. (2020) Preparation, characteristics, and antioxidant activities of carboxymethylated polysaccharides from blackcurrant fruits. *Int J Biol Macromol* 155: 1114–1122. <https://doi.org/10.1016/j.ijbiomac.2019.11.078>
10. Yu Y, Zhu SJ, Dong HT, et al. (2021) A novel MgF<sub>2</sub>/PDA/S-HA coating on the bio-degradable ZE21B alloy for better multi-functions on cardiovascular application. <https://doi.org/10.1016/j.jma.2021.06.015>
11. Wijesinghe WAJP, Jeon YJ (2012) Biological activities and potential industrial applications of fucose rich sulfated polysaccharides and fucoidans isolated from brown seaweeds: A review. *Carbohydr Polym* 88: 13–20. <https://doi.org/10.1016/j.carbpol.2011.12.029>
12. Lo TCT, Chang CA, Chiu KH, et al. (2011) Correlation evaluation of antioxidant properties on the monosaccharide components and glycosyl linkages of polysaccharide with different measuring methods. *Carbohydr Polym* 86: 320–327. <https://doi.org/10.1016/j.carbpol.2011.04.056>
13. Guerra-Dore CMP, Faustino Alves MG, Pofirio Will LSE, et al. (2013) A sulfated polysaccharide, fucans, isolated from brown algae *Sargassum vulgare* with anticoagulant, antithrombotic, antioxidant and anti-inflammatory effects. *Carbohydr Polym* 91: 467–475. <https://doi.org/10.1016/j.carbpol.2012.07.075>
14. Guillard RRL and Ryther JH (1962) Studies of marine planktonic diatoms: I. *Cyclotella Nana* Hustedt, and *Detonula Confervacea* (CLEVE) Gran. *Can J Microbiol* 8: 229–239. <https://doi.org/10.1139/m62-029>
15. Fimbres-Olivarria D, Lopez-Elias JA, Carvajal-Millan E, et al. (2016) *Navicula* sp. Sulfated polysaccharide gels induced by Fe(III): Rheology and microstructure. *Int J Mol Sci* 17: 1238. <https://doi.org/10.3390/ijms17081238>
16. Terho TT and Hartiala K (1971) Method for determination of the sulfate content of glycosaminoglycans. *Anal Biochem* 41: 471–476. [https://doi.org/10.1016/0003-2697\(71\)90167-9](https://doi.org/10.1016/0003-2697(71)90167-9)
17. AOAC (1995) Official Methods of Analysis of AOAC International, Washington DC, USA, Arlington, VA. Available from: [http://lib3.dss.go.th/fulltext/scan\\_ebook/aoac\\_1995\\_v78\\_n3.pdf](http://lib3.dss.go.th/fulltext/scan_ebook/aoac_1995_v78_n3.pdf).
18. Rouau X and Surget A (1994) A rapid semi-automated method for the determination of total and water-extractable pentosans in wheat flours. *Carbohydr Polym* 24: 123–132. [https://doi.org/10.1016/0144-8617\(94\)90022-1](https://doi.org/10.1016/0144-8617(94)90022-1)

19. Fimbres-Olivarria D, Carvajal-Millan E, Lopez-Elias JA, et al. (2018) Chemical characterization and antioxidant activity of sulfated polysaccharides from *Navicula* sp. *Food Hydrocoll* 75: 229–236. <https://doi.org/10.1016/j.foodhyd.2017.08.002>
20. Lee SY, Mediani A, Maulidiani M, et al. (2018) Comparison of partial least squares and random forests for evaluating relationship between phenolics and bioactivities of *Neptunia oleracea*. *J Sci Food Agric* 98: 240–252. <https://doi.org/10.1002/jsfa.8462>
21. Re R, Pellegrini N, Proteggenete A, et al. (1999) Antioxidant activity applying an improved ABTS radical cation decolorization assay. *Free Radic Biol Med* 26: 1231–1237. [https://doi.org/10.1016/S0891-5849\(98\)00315-3](https://doi.org/10.1016/S0891-5849(98)00315-3)
22. Benzie I and Strain J (1996) The ferric reducing ability of plasma (FRAP) as a measure of “antioxidant power”: The FRAP assay. *Anal Biochem* 239: 70–76. <https://doi.org/10.1006/abio.1996.0292>
23. López-Mata MA, Ruiz-Cruz S, Silva-Beltrán NP, et al. (2013) Physicochemical, antimicrobial and antioxidant properties of chitosan films incorporated with carvacrol. *Molecules* 18: 13735–13753. <https://doi.org/10.3390/molecules181113735>
24. Lynch EC (1990) Peripheral blood smear, In: Walker HK, Dallas WH, Hurst JW, *Clinical Methods: The History, Physical, and Laboratory Examinations*, Boston: Butterworth, 732–734.
25. D’Archivio AA, Maggi MA, Ruggieri F (2018) Extraction of curcuminoids by using ethyl lactate and its optimisation by response surface methodology. *J Pharm Biomed Anal* 149: 89–95. <https://doi.org/10.1016/j.jpba.2017.10.042>
26. Wiercigroch E, Szafraniec E, Czamara K, et al. (2017) Raman and infrared spectroscopy of carbohydrates: A review. *Spectrochim Acta - Part A Mol Biomol Spectrosc* 185: 317–335. <https://doi.org/10.1016/j.saa.2017.05.045>
27. Wang L, Wang X, Wu H, et al. (2014) Overview on biological activities and molecular characteristics of sulfated polysaccharides from marine green algae in recent years. *Mar Drugs* 12: 4984–5020. <https://doi.org/10.3390/md12094984>
28. Matsuhira B (1996) Vibrational spectroscopy of seaweed galactans. *Hydrobiologia* 326: 481–489. <https://doi.org/10.1007/BF00047849>
29. Barboríková J, Šutovská M, Kazimierová I, et al. (2019) Extracellular polysaccharide produced by *Chlorella vulgaris* – Chemical characterization and anti-asthmatic profile. *Int J Biol Macromol* 135: 1–11. <https://doi.org/10.1016/j.ijbiomac.2019.05.104>
30. Goo BG, Baek G, Jin Choi D, et al. (2013) Characterization of a renewable extracellular polysaccharide from defatted microalgae *Dunaliella tertiolecta*. *Bioresour Technol* 129: 343–350. <https://doi.org/10.1016/j.biortech.2012.11.077>
31. Huang SQ, Li JW, Li YQ, et al. (2011) Purification and structural characterization of a new water-soluble neutral polysaccharide GLP-F1-1 from *Ganoderma lucidum*. *Int J Biol Macromol* 48: 165–169. <https://doi.org/10.1016/j.ijbiomac.2010.10.015>
32. Rani RP, Anandharaj M, Ravindran A (2018) Characterization of a novel exopolysaccharide produced by *Lactobacillus gasser* FR4 and demonstration of its in vitro biological properties. *Int J Biol Macromol* 109: 772–783. <https://doi.org/10.1016/j.ijbiomac.2017.11.062>
33. Rajasekar P, Palanisamy S, Anjali R, et al. (2019) Isolation and structural characterization of sulfated polysaccharide from *Spirulina platensis* and its bioactive potential: In vitro antioxidant, antibacterial activity and Zebrafish growth and reproductive performance. *Int J Biol Macromol* 141: 809–821. <https://doi.org/10.1016/j.ijbiomac.2019.09.024>

34. Yuan F, Gao Z, Liu W, et al. (2019) Characterization, antioxidant, anti-aging and organ protective effects of sulfated polysaccharides from flammulina velutipes. *Molecules* 24: 3517. <https://doi.org/10.3390/molecules24193517>
35. Trabelsi I, Ben Slima S, Ktari N, et al. (2021) Structure analysis and antioxidant activity of a novel polysaccharide from katan seeds. *Biomed Res Int* 2021: 6349019. <https://doi.org/10.1155/2021/6349019>
36. Gurgel Rodrigues JA, Neto ÉM, dos Santos GRC, et al. (2014) Structural analysis of a sulfated polysaccharidic fraction obtained from the coenocytic green seaweed *Caulerpa cupressoides* var. *lycopodium*. *Acta Sci Technol* 36: 203–210. <https://doi.org/10.4025/actascitechnol.v36i2.17866>
37. Alencar POC, Lima GC, Barros FCN, et al. (2019) A novel antioxidant sulfated polysaccharide from the algae *Gracilaria caudata*: In vitro and in vivo activities. *Food Hydrocoll* 90: 28–34. <https://doi.org/10.1016/j.foodhyd.2018.12.007>
38. Wijesekara I, Pangestuti R, Kim SK (2011) Biological activities and potential health benefits of sulfated polysaccharides derived from marine algae. *Carbohydr Polym* 84: 14–21. <https://doi.org/10.1016/j.carbpol.2010.10.062>
39. Moore BG and Tischer RG (1964) Extracellular polysaccharides of algae: effects on life-support systems. *Science* 145: 586–587. <https://doi.org/10.1126/science.145.3632.586>
40. Raveendran S, Yoshida Y, Maekawa T, et al. (2013) Pharmaceutically versatile sulfated polysaccharide based bionano platforms. *Nanomed Nanotechnol Biol Med* 9: 605–626. <https://doi.org/10.1016/j.nano.2012.12.006>
41. Markou G and Nerantzis E (2013) Microalgae for high-value compounds and biofuels production: A review with focus on cultivation under stress conditions. *Biotechnol Adv* 31: 1532–1542. <https://doi.org/10.1016/j.biotechadv.2013.07.011>
42. Han PP, Sun Y, Jia SR, et al. (2014) Effects of light wavelengths on extracellular and capsular polysaccharide production by *Nostoc flagelliforme*. *Carbohydr Polym* 105: 145–151. <https://doi.org/10.1016/j.carbpol.2014.01.061>
43. Borowitzka MA, Beardall J, Raven JA (2016) The physiology of microalgae. <https://doi.org/10.1007/978-3-319-24945-2>
44. Lee JB, Hayashi K, Hirata M, et al. (2006) Antiviral sulfated polysaccharide from *Navicula directa*, a diatom collected from deep-sea water in toyama bay. *Biol Pharm Bull* 29: 2135–2139. <https://doi.org/10.1248/bpb.29.2135>
45. Khandeparker RD and Bhosle NB (2001) Extracellular polymeric substances of the marine fouling diatom *amphora rostrata* Wm.Sm. *Biofouling* 17: 117–127. <https://doi.org/10.1080/08927010109378471>
46. Sudharsan S, Subhapradha N, Seedeve P, et al. (2015) Antioxidant and anticoagulant activity of sulfated polysaccharide from *Gracilaria debilis* (Forsskal). *Int J Biol Macromol* 81: 1031–1038. <https://doi.org/10.1016/j.ijbiomac.2015.09.046>
47. Seedeve P, Moovendhan M, Viramani S, et al. (2017) Bioactive potential and structural characterization of sulfated polysaccharide from seaweed (*Gracilaria corticata*). *Carbohydr Polym* 155: 516–524. <https://doi.org/10.1016/j.carbpol.2016.09.011>
48. Leandro SM, Gil MC, Delgadillo I (2003) Partial characterisation of exopolysaccharides exuded by planktonic diatoms maintained in batch cultures. *Acta Oecologica* 24: 49–55. [https://doi.org/10.1016/S1146-609X\(03\)00004-3](https://doi.org/10.1016/S1146-609X(03)00004-3)



49. López-Mata MA, Ruiz-Cruz S, Silva-Beltrán NP, et al. (2015) Physicochemical and antioxidant properties of chitosan films incorporated with cinnamon Oil. *Int J Polym Sci* 2015: 974506. <https://doi.org/10.1155/2015/974506>
50. Majdoub H, Mansour M Ben, Chaubet F, et al. (2009) Anticoagulant activity of a sulfated polysaccharide from the green alga *Arthrospira platensis*. *Biochim Biophys Acta Gen Subj* 1790: 1377–1381. <https://doi.org/10.1016/j.bbagen.2009.07.013>
51. Zhang Z, Wang F, Wang X, et al. (2010) Extraction of the polysaccharides from five algae and their potential antioxidant activity in vitro. *Carbohydr Polym* 82: 118–121. <https://doi.org/10.1016/j.carbpol.2010.04.031>
52. Fedorov SN, Ermakova SP, Zvyagintseva TN, et al. (2013) Anticancer and cancer preventive properties of marine polysaccharides: Some results and prospects. *Mar Drugs* 11: 4876–4901. <https://doi.org/10.3390/md11124876>
53. Ale MT, Mikkelsen JD, Meyer AS (2011) Important determinants for fucoidan bioactivity: A critical review of structure-function relations and extraction methods for fucose-containing sulfated polysaccharides from brown seaweeds. *Mar Drugs* 9: 2106–2130. <https://doi.org/10.3390/md9102106>
54. Usov AI (2011) Chapter 4 - Polysaccharides of the red algae, In: Derek Horton, *Advances in Carbohydrate Chemistry and Biochemistry*, UK: Academic Press, 115–217. <https://doi.org/10.1016/B978-0-12-385520-6.00004-2>
55. Guo JH, Skinner GW, Harcum WW, et al. (1998) Pharmaceutical applications of naturally occurring water-soluble polymers. *Pharm Sci Technol Today* 1: 254–261. [https://doi.org/10.1016/S1461-5347\(98\)00072-8](https://doi.org/10.1016/S1461-5347(98)00072-8)
56. Melo MRS, Feitosa JPA, Freitas ALP, et al. (2002) Isolation and characterization of soluble sulfated polysaccharide from the red seaweed *Gracilaria cornea*. *Carbohydr Polym* 49: 491–498. [https://doi.org/10.1016/S0144-8617\(02\)00006-1](https://doi.org/10.1016/S0144-8617(02)00006-1)
57. Rengasamy KR, Mahomoodally MF, Aumeeruddy MZ, et al. (2020) Bioactive compounds in seaweeds: An overview of their biological properties and safety. *Food Chem Toxicol* 135: 111013. <https://doi.org/10.1016/j.fct.2019.111013>
58. Barros FCN, Da Silva DC, Sombra VG, et al. (2013) Structural characterization of polysaccharide obtained from red seaweed *Gracilaria caudata* (J Agardh). *Carbohydr Polym* 92: 598–603. <https://doi.org/10.1016/j.carbpol.2012.09.009>
59. Ale MT, Maruyama H, Tamauchi H, et al. (2011) Fucose-containing sulfated polysaccharides from brown seaweeds inhibit proliferation of melanoma cells and induce apoptosis by activation of caspase-3 in vitro. *Mar Drugs* 9: 2605–2621. <https://doi.org/10.3390/md9122605>
60. Patel S (2012) Therapeutic importance of sulfated polysaccharides from seaweeds: updating the recent findings. *3 Biotech* 2: 171–185. <https://doi.org/10.1007/s13205-012-0061-9>
61. Chen C, Zhao Z, Ma S, et al. (2019) Optimization of ultrasonic-assisted extraction, refinement and characterization of water-soluble polysaccharide from *Dictyosphaerium* sp. and evaluation of antioxidant activity in vitro. *J Food Meas Charact* 14: 963–977. <https://doi.org/10.1007/s11694-019-00346-7>
62. Kan Y, Chen T, Wu Y, et al. (2015) Antioxidant activity of polysaccharide extracted from *Ganoderma lucidum* using response surface methodology. *Int J Biol Macromol* 72: 151–157. <https://doi.org/10.1016/j.ijbiomac.2014.07.056>

63. Gómez-Ordóñez E, Jiménez-Escrig A, Rupérez P (2014) Bioactivity of sulfated polysaccharides from the edible red seaweed *Mastocarpus stellatus*. *Bioact Carbohydrates Diet Fibre* 3: 29–40. <https://doi.org/10.1016/j.bcdf.2014.01.002>
64. Yarnpakdee S, Benjakul S, Senphan T (2019) Antioxidant activity of the extracts from freshwater macroalgae (*Cladophora glomerata*) grown in Northern Thailand and its preventive effect against lipid oxidation of refrigerated eastern little tuna slice. *Turkish J Fish Aquat Sci* 19: 209–219. [https://doi.org/10.4194/1303-2712-v19\\_03\\_04](https://doi.org/10.4194/1303-2712-v19_03_04)
65. Wang J, Hu S, Nie S, et al. (2016) Reviews on mechanisms of in vitro antioxidant activity of polysaccharides. *Oxid Med Cell Longev* 2016: 5692852. <https://doi.org/10.1155/2016/5692852>
66. de Oliveira FC, Coimbra JS dos R, de Oliveira EB, et al. (2016) Food Protein-polysaccharide Conjugates Obtained via the Maillard Reaction: A Review. *Crit Rev Food Sci Nutr* 56: 1108–1125. <https://doi.org/10.1080/10408398.2012.755669>
67. Alisi IO, Uzairu A, Abechi SE (2020) Free radical scavenging mechanism of 1,3,4-oxadiazole derivatives: thermodynamics of O–H and N–H bond cleavage. *Heliyon* 6: e03683. <https://doi.org/10.1016/j.heliyon.2020.e03683>
68. El Kady EM (2019) New Trends of the Polysaccharides as a Drug. *World J Agric Soil Sci* 3: 1–22. <https://doi.org/10.33552/wjass.2019.03.000572>
69. Li H, Mao W, Zhang X, et al. (2011) Structural characterization of an anticoagulant-active sulfated polysaccharide isolated from green alga *Monostroma latissimum*. *Carbohydr Polym* 85: 394–400. <https://doi.org/10.1016/j.carbpol.2011.02.042>
70. Guru SMM, Vasanthi M, Achary A (2015) Antioxidant and free radical scavenging potential of crude sulphated polysaccharides from *Turbinaria ornata*. *Biologia (Bratisl)* 70: 27–33. <https://doi.org/10.1515/biolog-2015-0004>
71. Shao P, Chen X, Sun P (2014) Chemical characterization, antioxidant and antitumor activity of sulfated polysaccharide from *Sargassum horneri*. *Carbohydr Polym* 105: 260–269. <https://doi.org/10.1016/j.carbpol.2014.01.073>
72. Cao M, Wang S, Gao Y, et al. (2020) Study on physicochemical properties and antioxidant activity of polysaccharides from *Desmodesmus armatus*. *J Food Biochem* 44: 1–13. <https://doi.org/10.1111/jfbc.13243>
73. Díaz-Gutierrez D, Méndez Ortega W, de Oliveira e Silva AM, et al. (2015) Comparison of antioxidants properties and polyphenols content of aqueous extract from seaweeds *Bryothamnion triquetrum* and *Halimeda opuntia*. *Ars Pharm* 56: 89–99. <https://doi.org/10.4321/S2340-98942015000200003>
74. Khalili M, Ebrahimzadeh MA, Safdari Y (2014) Antihemolytic activity of thirty herbal extracts in mouse red blood cells. *Arch Ind Hyg Toxicol* 65: 399–406. <https://doi.org/10.2478/10004-1254-65-2014-2513>
75. Hernández-Ruiz KL, Ruiz-Cruz S, Cira-Chávez LA, et al. (2018) Evaluation of antioxidant capacity, protective effect on human erythrocytes and phenolic compound identification in two varieties of plum fruit (*Spondias* spp.) by UPLC-MS. *Molecules* 23: 3200. <https://doi.org/10.3390/molecules23123200>
76. García-Romo JS, Noguera-Artiaga L, Gálvez-Irriqui AC, et al. (2020) Antioxidant, antihemolysis, and retinoprotective potentials of bioactive lipidic compounds from wild shrimp (*Litopenaeus stylirostris*) muscle. *CYTA-J Food* 18: 153–163. <https://doi.org/10.1080/19476337.2020.1719210>

77. Liu RH and Finley J (2005) Potential cell culture models for antioxidant research. *J Agric Food Chem* 53: 4311–4314. <https://doi.org/10.1021/jf058070i>
78. Babu BH, Shylesh BS, Padikkala J (2001) Antioxidant and hepatoprotective effect of *Acanthus ilicifolius*. *Fitoterapia* 72: 272–277. [https://doi.org/10.1016/S0367-326X\(00\)00300-2](https://doi.org/10.1016/S0367-326X(00)00300-2)
79. Finkel T and Holbrook NJ (2000) Oxidants, oxidative stress and the biology of ageing. *Nature* 408: 239–247. <https://doi.org/10.1038/35041687>
80. Ingrosso D, D'Angelo S, di Carlo E, et al. (2000) Increased methyl esterification of altered aspartyl residues erythrocyte membrane proteins in response to oxidative stress. *Eur J Biochem* 267: 4397–4405. <https://doi.org/10.1046/j.1432-1327.2000.01485.x>
81. Prior RL, Wu X, Schaich K (2005) Standardized methods for the determination of antioxidant capacity and phenolics in foods and dietary supplements. *J Agric Food Chem* 53: 4290–4302. <https://doi.org/10.1021/jf0502698>



AIMS Press

© 2022 the Author(s), licensee AIMS Press. This is an open access article distributed under the terms of the Creative Commons Attribution License (<http://creativecommons.org/licenses/by/4.0>)